Mathematical Biosciences 315 (2019) 108216

Contents lists available at ScienceDirect

Mathematical Biosciences

journal homepage: www.elsevier.com/locate/mbs

Drug delivery from microcapsules: How can we estimate the release time?

Elliot J. Carr*[,a], Giuseppe Pontrelli[b]

[a] School of Mathematical Sciences, Queensland University of Technology (QUT), Brisbane, Australia
[b] Istituto per le Applicazioni del Calcolo-CNR, Via dei Taurini 19 Rome 00185, Italy

ARTICLE INFO

Keywords:
Mass diffusion
Drug release
Release time
Composite capsule
Asymptotic estimates

ABSTRACT

Predicting the release performance of a drug delivery device is an important challenge in pharmaceutics and biomedical science. In this paper, we consider a multi-layer diffusion model of drug release from a composite spherical microcapsule into an external surrounding medium. Based on this model, we present two approaches for estimating the release time, i.e. the time required for the drug-filled capsule to be depleted. Both approaches make use of temporal moments of the drug concentration at the centre of the capsule, which provide useful insight into the timescale of the process and can be computed exactly without explicit calculation of the full transient solution of the multi-layer diffusion model. The first approach, which uses the zeroth and first temporal moments only, provides a crude approximation of the release time taking the form of a simple algebraic expression involving the various parameters in the model (e.g. layer diffusivities, mass transfer coefficients, partition coefficients) while the second approach yields an asymptotic estimate of the release time that depends on consecutive higher moments. Through several test cases, we show that both approaches provide a computationally-cheap and useful tool to quantify the release time of composite microcapsule configurations.

1. Introduction

Polymeric microcapsules are commonly used in pharmaceutical or medical processes as drug carriers or for the encapsulation of organic cells [1,2]. The main functions of these micro- or nano-sized vesicles are the efficient transport and controlled release of the therapeutic agent into the external environment. Typically, drug-filled microcapsules exhibit a multi-layered structure consisting of a spherical core surrounded by a thin, protective semi-permeable polymeric shell. The release properties depend crucially on the nature of this coating structure [3]. For this reason, in recent years, materials innovation and nanotechnology have stimulated novel research and progress in biodegradable, biocompatible, environment-responsive, and targeted delivery systems [4,5]. Mathematical modeling plays an important role in elucidating the drug release mechanisms, thus facilitating the development of advanced materials and the assessment of smart products by a systematic, rather than trial-and-error, approach. Within this area, special attention is given to semi-empirical and mechanistic models, which often provide a good fit with experimental data [6,7].

Analysis and solution of mechanistic models taking into account the multi-layer structure of the microcapsule has been recently addressed by Kaoui et al. [8] and Carr and Pontrelli [9]. However, even when the drug diffusion process is well represented mathematically, analytical tools or simple indicators remain useful for extracting insight from the model and the data. Such tools allow practical questions to be answered, such as how long does it takes to attain a steady state or therapeutic flux, or what parameters need to be adjusted and by how much, in order to achieve a certain delivery rate without solving the complete mechanistic model. Furthermore, when a full mathematical representation is unavailable, or is too complicated to use in practice, simple performance indicators can identify the main transport mechanisms and the most important components of the process. In most circumstances, for example, rather than the full transient solution, the time required to reach a steady state plasma drug concentration solely determines the effectiveness of the delivery system.

For control systems analysis, Laplace transform and linearization techniques are commonly used to describe the dynamics of the process via an effective time constant [10], which represents a useful indicator of the time required to attain steady state. The concept of a time constant is crucial to pharmaceutical developers who want to create controlled-release devices able to deliver drugs at a desired rate. Estimation of the *release time*, i.e. the time required for the drug-filled capsule to be depleted, is of great importance in the design of drug delivery systems, because it allows product manufacturers to adjust certain properties to ensure a precise release within a determined time [11]. The idea of using a single timescale to characterize how fast the drug concentration

* Corresponding author.
E-mail address: elliot.carr@qut.edu.au (E.J. Carr).

https://doi.org/10.1016/j.mbs.2019.108216
Received 24 January 2019; Received in revised form 12 April 2019; Accepted 13 June 2019
Available online 18 June 2019

reaches the equilibrium value has been explored by several authors. Pontrelli and Simon [12] define a timescale equal to the mean of a normalized probability density function representing the transition of the concentration profile from initial to equilibrium state. Calculating this mean requires either computing the full transient solution or evaluating the Laplace transform of the transient solution, and ultimately for multi-layered problems, produces quite complex expressions for the timescale in terms of the relevant parameters in the model. Another approach is the concept of mean action time, which has been used to characterize how long a diffusion process takes to reach steady state [13–16]. Here, the transition from initial to equilibrium state is represented as a cumulative distribution function, with the mean of the corresponding probability density function defining the characteristic timescale. The attraction of the mean action time is that it completely avoids any calculation of the transient solution and produces simple explicit algebraic formulas for the timescale in terms of the parameters in the model [14,15]. Finally, we note that the notion of release time is different but related to the concept of penetration time, which that has been studied in a number of configurations for thermal disturbances in heat conduction problems [17].

In this paper, inspired by recent literature on diffusion processes [14,15,18–20], we present two approaches for estimating the release time for a drug-filled capsule. Both approaches utilize temporal moments of the concentration versus time curve at the centre of the capsule. The first approach, which uses the zeroth and first moments only, provides a crude approximation of the release time expressed in terms of the various parameters in the model (e.g. layer diffusivities, mass transfer coefficients, partition coefficients). The second approach yields an asymptotic estimate of the release time, defined as the time when the drug concentration at the centre of the capsule is a small prescribed distance away from its steady-state value. Attractively, both approaches can be used without explicit (analytical or numerical) solution of the underlying mathematical model.

The remaining parts of this article are ordered in the following way: (i) the diffusion model for drug release from a spherical multi-layer capsule is presented (ii) both approaches for quantifying the release time are described (iii) a specific case study on a core-shell capsule is considered and numerical results presented and discussed.

2. Drug diffusion model for a multi-layer sphere

Multi-layer capsules consist of a drug-loaded (fluid or solid) spherical core surrounded by one or more polymeric layers [1,2]. Such layer-by-layer assembly enhances a selective diffusion and allows for better control of the transfer rate. In this framework, and in the most general case of n layers, the composite system can be treated as a sequence of enveloping concentric shells, constituted by spheres of increasing radii satisfying $0 < R_0 < R_1 < \cdots < R_n$ (see Fig. 1 for the case $n = 1$). The capsule's outermost layer is protected by a thin semi-permeable coating that shields and preserves the encapsulated drug from degradation and chemical aggression, protects the inner structure, and guarantees a more controlled and sustained release [21]. The coating is in contact with the targeted external release medium (either a bulk fluid or a tissue). Strictly speaking, for a pure diffusion problem in a homogeneous medium, the concentration field decays exponentially and reaches zero at infinite distance [22]. Nevertheless, for computational purposes, we can confine the diffusion process within an enveloping spherical layer of finite extent, at a distance far away from the capsule surface. In our model, this additional layer is defined by setting a cut-off radius $R_\infty \gg R_n$ (sometimes named *release distance* or *diffusion length*), beyond which the concentration is effectively zero at all times (Fig. 1) [23]:

$$c(x, t) \simeq 0 \qquad \text{for all } x \geq R_\infty \text{ and } t > 0.$$

Under the assumptions of homogeneity and isotropy, we can consider a one-dimensional model (Fig. 1) with radial symmetry. We adopt

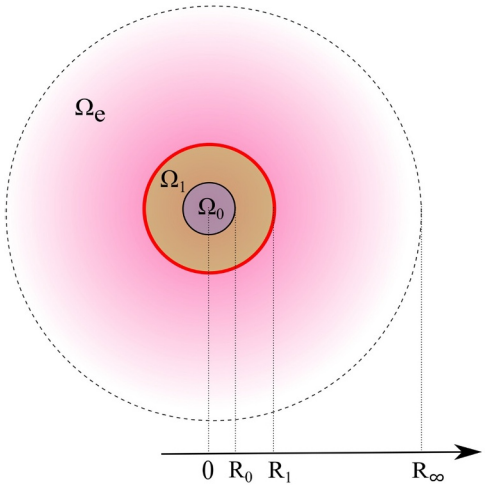

Fig. 1. Schematic representation of the cross-section of the radially symmetric capsule, comprising an internal core Ω_0 $(0 < r < R_0)$, a concentric layer Ω_1 $(R_0 < r < R_1)$ and the thin coating shell (in red). This two-layer sphere is immersed in the release medium, represented by a concentric external layer Ω_e, delimited by the dashed line R_∞. The length R_∞ is named *release distance* and is defined as the minimum distance from the sphere surface beyond which $c(x, t) \simeq 0$, within a prescribed tolerance, at all times. This three enveloped layer system constitutes the object of our modelling (figure not to scale). (For interpretation of the references to colour in this figure, the reader is referred to the web version of this article.)

the model formulated in [8,9], where the evolution of concentrations in the layers is governed by a set of one-dimensional linear diffusion equations:

$$\frac{\partial c_0}{\partial t} = \frac{D_0}{r^2}\frac{\partial}{\partial r}\left(r^2\frac{\partial c_0}{\partial r}\right), \quad r \in (0, R_0), \tag{2.1}$$

$$\frac{\partial c_i}{\partial t} = \frac{D_i}{r^2}\frac{\partial}{\partial r}\left(r^2\frac{\partial c_i}{\partial r}\right), \quad r \in (R_{i-1}, R_i) \text{ for } i = 1, \ldots, n, \tag{2.2}$$

$$\frac{\partial c_e}{\partial t} = \frac{D_e}{r^2}\frac{\partial}{\partial r}\left(r^2\frac{\partial c_e}{\partial r}\right), \quad r \in (R_n, R_\infty), \tag{2.3}$$

paired with interlayer and boundary conditions

$$\frac{\partial c_0}{\partial r} = 0, \quad r = 0, \tag{2.4}$$

$$c_i = \sigma_i c_{i+1}, \quad D_i\frac{\partial c_i}{\partial r} = D_{i+1}\frac{\partial c_{i+1}}{\partial r}, \quad r = R_i \text{ for } i = 0, 1, \ldots, n-1, \tag{2.5}$$

$$D_n\frac{\partial c_n}{\partial r} = D_e\frac{\partial c_e}{\partial r}, \quad D_e\frac{\partial c_e}{\partial r} = P(\sigma_n c_e - c_n), \quad r = R_n, \tag{2.6}$$

$$c_e = 0, \quad r = R_\infty. \tag{2.7}$$

In the above equations, the parameters D_i are the diffusion coefficients of drug in each layer, σ_i are the partition coefficients, and P is the mass transfer coefficient at the external coating [8,9]. For a releasing drug-loaded core, the initial conditions are:

$$c_0(r, 0) = C_0, \quad r \in (0, R_0), \tag{2.8}$$

$$c_i(r, 0) = 0, \quad r \in (R_{i-1}, R_i) \text{ for } i = 1, \ldots, n, \tag{2.9}$$

$$c_e(r, 0) = 0, \quad r \in (R_n, R_\infty), \tag{2.10}$$

where $C_0 > 0$ is a constant. The steady state solution of the drug diffusion model (2.1)–(2.10) is trivially given by

$$c_i^\infty(r) = \lim_{t\to\infty} c_i(r) = 0, \qquad \text{for} \quad i = 0, 1, \ldots, n, e. \tag{2.11}$$

In our previous studies the transient solution of Eqs. (2.1)–(2.10) was obtained through a separation of variables [8], or a Laplace transform

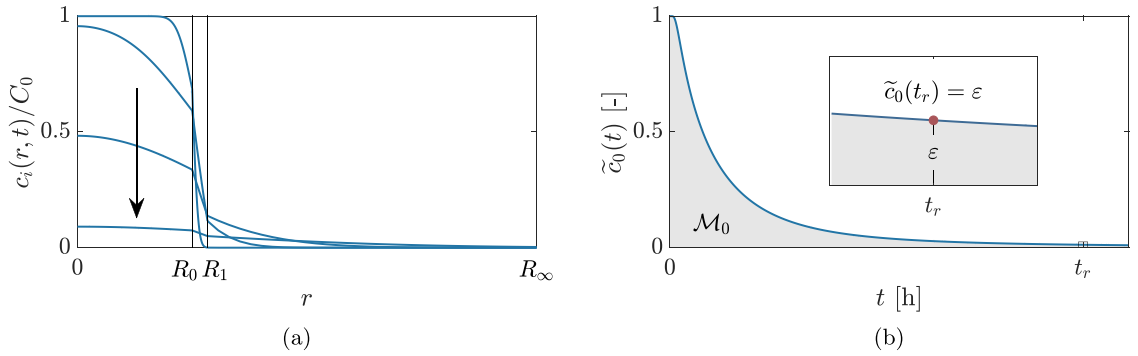

Fig. 2. Typical spatio-temporal behaviour of the drug concentration arising from the drug diffusion model (2.1)–(2.10) with a single hydrogel layer ($n = 1$) (a) Plot of the dimensionless concentration, $c_i(r, t)/C_0$, versus radius r at four values of t with a black arrow indicating the direction of increasing time. Vertical lines denote the interfaces $r = R_0$ and $r = R_1$. (b) Plot of the dimensionless concentration at the centre of the capsule $\tilde{c}_0(t)$ versus time. The shaded area underneath this curve defines the zeroth moment $\mathcal{M}_0$ (3.2) while the release time, as defined in Eq. (3.1), is the time when $\tilde{c}_0(t)$ reaches a small prescribed value ε.

approach [9]. In some circumstances, however, rather than working with the complicated expressions of the full solution, simple and cheap measures of the performance of the delivery system are desired. In the following sections, we propose two ways to quantify the *release time* of the microcapsule, that is, the time taken for the capsule to be depleted of the drug.

3. Crude approximation of the release time

Fig. 2 shows the typical spatio-temporal behaviour of the dimensionless concentration, $c_i(r, t)/C_0$, arising from the solution of the diffusion model (2.1)–(2.10). An important observation from this plot is that the centre of the capsule, $r = 0$, takes the longest time to reach steady state. In Fig. 2b we plot the dimensionless concentration at the centre of the capsule, $\tilde{c}_0(t) := c_0(0, t)/C_0$, versus time as it progresses towards the steady state solution of zero concentration (2.11). Using the curve $\tilde{c}_0(t)$ we define the release time, as the time $t_r > 0$ satisfying:

$$\tilde{c}_0(t_r) = \varepsilon, \tag{3.1}$$

where ε is a small specified tolerance (see Fig. 2b) [18,20]. In other words, t_r measures the time taken for the capsule to be depleted within a small tolerance. Since $\tilde{c}_0(t)$ monotonically decreases from one to zero, t_r is unique for a given choice of ε. Under this definition, the release time is not an absolute concept, but dependent on the desired level of accuracy required to measure a complete depletion.

We now define a crude approximation of the release time t_r (3.1) based on temporal moments of $\tilde{c}_0(t)$. The area underneath the curve $\tilde{c}_0(t)$, or the zeroth temporal moment of $\tilde{c}_0(t)$, shaded in Fig. 2b, is defined as

$$\mathcal{M}_0 = \int_0^\infty \tilde{c}_0(t)\,\mathrm{d}t. \tag{3.2}$$

The value of $\mathcal{M}_0$ will tend to be small for a fast release and large for a slow release. Moreover, when comparing two different capsule configurations, if the corresponding $\tilde{c}_0(t)$ curves for the two configurations do not intersect then the configuration with the larger release time will have a larger area (larger value of $\mathcal{M}_0$). Therefore, it is reasonable to conclude that $\mathcal{M}_0$ provides a useful characterization of the timescale of release[1].

A major attraction of working with Eq. (3.2) is that a simple closed-form expression can be derived for $\mathcal{M}_0$ involving the model parameters without requiring the full analytical or numerical solution expression for $c_0(0, t)$. This is achieved by extending and modifying similar ideas presented elsewhere (see, e.g., [14,15]). First, we define:

$$u_i(r) = \frac{1}{C_0}\int_0^\infty c_i(r, t)\,\mathrm{d}t, \tag{3.3}$$

which allow us to write down an equivalent form of Eq. (3.2)

$$\mathcal{M}_0 = u_0(0). \tag{3.4}$$

Next, applying the linear operator $\mathcal{L}$, defined as

$$\mathcal{L}\varphi := \frac{D_i}{r^2}\frac{\mathrm{d}}{\mathrm{d}r}\left(r^2\frac{\mathrm{d}\varphi}{\mathrm{d}r}\right), \tag{3.5}$$

to both sides of Eq. (3.3) and making use of Eqs. (2.1)–(2.3) yields the following differential equation:

$$\frac{D_i}{r^2}\frac{\mathrm{d}}{\mathrm{d}r}\left(r^2\frac{\mathrm{d}u_i}{\mathrm{d}r}\right) = \frac{1}{C_0}[c_i^\infty(r) - c_i(r, 0)]. \tag{3.6}$$

Supplementary boundary and interlayer conditions corresponding to Eqs. (2.4)–(2.7) are derived using the definition of $u_i(r)$ in Eq. (3.3) (see, e.g. [14,18]). In summary, recalling the initial conditions (2.8)–(2.10) and the steady-state solution (2.11), we have the following boundary value problem satisfied by $u_i(r)$ ($i = 0, 1, \ldots, n, e$):

$$\frac{D_0}{r^2}\frac{\mathrm{d}}{\mathrm{d}r}\left(r^2\frac{\mathrm{d}u_0}{\mathrm{d}r}\right) = -1, \quad r \in (0, R_0) \tag{3.7}$$

$$\frac{D_i}{r^2}\frac{\mathrm{d}}{\mathrm{d}r}\left(r^2\frac{\mathrm{d}u_i}{\mathrm{d}r}\right) = 0, \quad r \in (R_{i-1}, R_i) \text{ for } i = 1, \ldots, n, \tag{3.8}$$

$$\frac{D_e}{r^2}\frac{\mathrm{d}}{\mathrm{d}r}\left(r^2\frac{\mathrm{d}u_e}{\mathrm{d}r}\right) = 0, \quad r \in (R_n, R_\infty), \tag{3.9}$$

$$\frac{\mathrm{d}u_0}{\mathrm{d}r} = 0, \quad r = 0, \tag{3.10}$$

$$u_i = \sigma_i u_{i+1}, \quad D_i\frac{\mathrm{d}u_i}{\mathrm{d}r} = D_{i+1}\frac{\mathrm{d}u_{i+1}}{\mathrm{d}r}, \quad r = R_i \text{ for } i = 0, 1, \ldots, n-1, \tag{3.11}$$

$$D_n\frac{\mathrm{d}u_n}{\mathrm{d}r} = D_e\frac{\mathrm{d}u_e}{\mathrm{d}r}, \quad D_e\frac{\mathrm{d}u_e}{\mathrm{d}r} = P(\sigma_n u_e - u_n), \quad r = R_n, \tag{3.12}$$

$$u_e = 0, \quad r = R_\infty. \tag{3.13}$$

The above boundary value problem admits a closed-form analytical solution. By way of example, we consider the simplest case of the *core-shell model*, a drug-filled core surrounded by one hydrogel shell ($n = 1$). In this case, the differential Eqs. (3.7)–(3.9) possess the general solution:

$$u_0(r) = \frac{\alpha_0}{r} + \alpha_1 - \frac{r^2}{6D_0}, \tag{3.14}$$

[1] We remark that Eq. (3.2) differs from the standard definition of mean action time (see e.g. [14]) commonly used to characterize the time taken for a diffusion process to reach steady state. The reason for this difference is that the standard definition is not defined when $c_i(r, 0) = c_i^\infty(r)$, as is the case in Eqs. (2.9)–(2.11).

$$u_1(r) = \frac{\alpha_2}{r} + \alpha_3, \tag{3.15}$$

$$u_e(r) = \frac{\alpha_4}{r} + \alpha_5, \tag{3.16}$$

where α_0, α_1, ..., α_5 are arbitrary constants. Immediately, the boundary condition (3.10) requires $\alpha_0 = 0$. The remaining constants satisfy the following algebraic system generated by substituting Eqs. (3.14)–(3.16) into the four interface conditions (3.11)–(3.12) with $n = 1$:

$$\alpha_1 - \frac{R_0^2}{6D_0} = \sigma_0\left(\frac{\alpha_2}{R_0} + \alpha_3\right), \tag{3.17}$$

$$\frac{R_0}{3} = \frac{D_1\alpha_2}{R_0^2}, \tag{3.18}$$

$$\frac{D_1\alpha_2}{R_1^2} = \frac{D_e\alpha_4}{R_1^2}, \tag{3.19}$$

$$-\frac{D_e\alpha_4}{R_1^2 P} = \sigma_1\left(\frac{\alpha_4}{R_1} + \alpha_5\right) - \frac{\alpha_2}{R_1} - \alpha_3, \tag{3.20}$$

$$\frac{\alpha_4}{R_\infty} + \alpha_5 = 0. \tag{3.21}$$

Eqs. (3.17)–(3.21) can then be solved sequentially: Eq. (3.18) for α_2, Eq. (3.19) for α_4, Eq. (3.21) for α_5, Eq. (3.20) for α_3 and finally Eq. (3.17) for α_1. Combining these results with Eqs. (3.14)–(3.16) yields the solution to the boundary value problem (3.7)–(3.13)[2]:

$$u_0(r) = \frac{R_0^2 - r^2}{6D_0} + \frac{\sigma_0 R_0^2(R_1 - R_0)}{3D_1R_1} + \frac{\sigma_0\sigma_1 R_0^3(R_\infty - R_1)}{3D_eR_1R_\infty} + \frac{\sigma_0 R_0^3}{3R_1^2P}, \tag{3.22}$$

$$u_1(r) = \frac{R_0^3(r - R_1)}{3D_1R_1r} + \frac{\sigma_1 R_0^3(R_\infty - R_1)}{3D_eR_1R_\infty} + \frac{R_0^3}{3R_1^2P}, \tag{3.23}$$

$$u_e(r) = \frac{R_0^3(R_\infty - r)}{3D_eR_\infty r}. \tag{3.24}$$

Evaluating Eq. (3.22) at $r = 0$ gives the following expression for the zeroth moment (3.4):

$$\mathcal{M}_0 = \frac{R_0^2}{6D_0} + \frac{\sigma_0 R_0^2(R_1 - R_0)}{3D_1R_1} + \frac{\sigma_0\sigma_1 R_0^3(R_\infty - R_1)}{3D_eR_1R_\infty} + \frac{\sigma_0 R_0^3}{3R_1^2P}. \tag{3.25}$$

In summary, Eq. (3.25) provides a simple formula for characterizing the timescale of release: for small values of $\mathcal{M}_0$ we expect a rapid release while for large values of $\mathcal{M}_0$ we expect a slow release.

To approximate the release time t_r (3.1) we incorporate the first temporal moment, $\mathcal{M}_1 = \int_0^\infty t\,\tilde{c}_0(t)\,dt$, into the calculation:

$$t_r \simeq \mathcal{M}_0 + 3\sqrt{\mathcal{M}_1} =: \hat{t}_r, \tag{3.26}$$

where the square root ensures that the second term has units of time. The inclusion of the first moment introduces a penalty to $\tilde{c}_0(t)$ curves with heavy tails that exhibit a slower decay to zero, behaviour that may not be captured by the zeroth moment alone. The formula (3.26) follows a similar approximation used by Simpson et al. [15] for estimating response times of groundwater diffusion processes while the coefficient of three is a heuristic factor inspired by the three sigma rule [24]. By deriving a similar boundary value problem to Eqs. (3.7)–(3.13) for the first moment, $\mathcal{M}_1$, as described later in Section 4, the following closed-form expression can be derived:

$$\begin{aligned} t_r \simeq\ & \frac{R_0^2}{6D_0} + \frac{\sigma_0 R_0^2(R_1 - R_0)}{3D_1R_1} + \frac{\sigma_0\sigma_1 R_0^3(R_\infty - R_1)}{3D_eR_1R_\infty} + \frac{\sigma_0 R_0^3}{3R_1^2P} \\ & + 3\left\{\frac{7R_0^4}{180D_0^2} + \frac{7\sigma_0 R_0^4(R_1 - R_0)}{45D_0D_1R_1} + \frac{7\sigma_0\sigma_1 R_0^5(R_\infty - R_1)}{45D_0D_eR_1R_\infty} + \frac{7\sigma_0 R_0^5}{45D_0PR_1^2}\right. \\ & + \frac{2\sigma_0 R_0^3(R_1 - R_0)^2(\sigma_0R_0 + R_1 - R_0)}{9D_1^2R_1^2} + \frac{4\sigma_0\sigma_1 R_0^3(R_\infty - R_1)(\sigma_0R_0^3 - R_0^3 + R_1^3)}{9D_ePR_1^3R_\infty} \\ & + \frac{2\sigma_0 R_0^3(R_1 - R_0)(2\sigma_0R_0^2 - 2R_0^2 + R_0R_1 + R_1^2)}{9D_1R_1^2} \times \left[\frac{\sigma_1(R_\infty - R_1)}{D_eR_\infty} + \frac{1}{PR_1}\right] \\ & \left. + \frac{2\sigma_0\sigma_1 R_0^3(R_\infty - R_1)^2(\sigma_0\sigma_1R_0^3 - \sigma_1R_0^3 + \sigma_1R_1^3 - R_1^3 + R_1^2R_\infty)}{9D_e^2R_1^2R_\infty^2}\right\}^{1/2}. \end{aligned} \tag{3.27}$$

The advantage of incorporating information about the first moment is that the expression (3.27), although more complex and costly than (3.25), provides a better estimate of the release time (see Section 5 for additional comments on the results). Other estimates can be defined by modifying (3.26) to include higher moments, but because of their increasingly complicated form, they likely have limited practical use.

In the next section, we present an iterative procedure to improve the estimate of t_r.

4. Estimating the release time using high order moments

Eq. (3.27) provides a crude approximation of the release time of the capsule, t_r, as defined in Eq. (3.1). In this section, we present a highly-accurate asymptotic estimate of t_r by extending, to multi-layer diffusion in spherical coordinates, previous work by Carr [18], which focussed on monolayer diffusion in Cartesian coordinates. At $r = 0$, the analytical solution to the drug diffusion model (2.1)–(2.10) possesses the following functional form [8]:

$$\tilde{c}_0(t) = \sum_{j=0}^{\infty} \gamma_j e^{-t\beta_j}, \quad 0 < \beta_0 < \beta_1 < \beta_2 < \cdots, \tag{4.1}$$

where γ_j and β_j are constants. It follows then that the long time behaviour of the concentration is exponentially decreasing:

$$\tilde{c}_0(t) \simeq \gamma_0 e^{-t\beta_0}, \quad \text{as } t \to \infty. \tag{4.2}$$

Combining Eqs. (3.1) and (4.2) gives the following asymptotic estimate of the release time[3]:

$$t_r \simeq \frac{\ln(\gamma_0/\varepsilon)}{\beta_0}. \tag{4.3}$$

The formula (4.3) requires knowledge of γ_0 and β_0, which are related to the dominant eigenvalue and eigenfunction pair of the underlying Sturm-Liouville problem [8]. Alternatively, γ_0 and β_0 can be calculated by using appropriate temporal moments of the concentration [18] as we now describe. Define the kth temporal moment:

$$\mathcal{M}_k = \int_0^\infty t^k\,\tilde{c}_0(t)\,dt, \tag{4.4}$$

and let

$$u_{i,k}(r) = \frac{1}{C_0}\int_0^\infty t^k c_i(r, t)\,dt, \tag{4.5}$$

where the first subscript indicates the layer ($i = 0, 1, ..., e$) and the second subscript denotes the kth moment ($k = 0, 1, ...$). Combining Eqs. (4.1) and (4.4) and carrying out the integration yields:

$$\mathcal{M}_k = \sum_{j=0}^{\infty} \frac{k!\gamma_j}{\beta_j^{k+1}}. \tag{4.6}$$

Since $\beta_0 < \beta_j$ for all $j = 1, 2, ...$, we have the following asymptotic expression for the higher moments [18]:

[2] Note that evaluating either $u_0(r)$, $u_1(r)$ or $u_e(r)$ allows the area under the $\tilde{c}_0(t)$ curve between $t = 0$ and $t \to \infty$ to be calculated for any value of r, which may also be of practical interest.

[3] To guarantee $t_r > 0$, the condition $\varepsilon < \gamma_0$ is required.

$$\mathcal{M}_k \simeq \frac{k!\,\gamma_0}{\beta_0^{k+1}}, \quad \text{as } k \to \infty. \tag{4.7}$$

Evaluating Eq. (4.7) at k and $k-1$ and solving the resulting algebraic system for γ_0 and β_0 gives:

$$\gamma_0 = \frac{\mathcal{M}_k}{k!}\left(\frac{k\mathcal{M}_{k-1}}{\mathcal{M}_k}\right)^{k+1}, \quad \beta_0 = \frac{k\mathcal{M}_{k-1}}{\mathcal{M}_k}. \tag{4.8}$$

Finally, substituting Eq. (4.8) into Eq. (4.3) yields the following asymptotic estimate of the release time:

$$t_r \simeq \frac{\mathcal{M}_k}{k\mathcal{M}_{k-1}} \ln\left[\frac{\mathcal{M}_k}{k!\,\varepsilon}\left(\frac{k\mathcal{M}_{k-1}}{\mathcal{M}_k}\right)^k\right] =: t_r^*, \tag{4.9}$$

where the superscript (*) is used to signify that t_r^* is an asymptotic estimate of t_r. Due to Eq. (4.7), t_r^* becomes more accurate for large k [18]. The attraction of the formula for t_r^* is that the moment expressions appearing in Eq. (4.9) can be calculated without computing the full transient solution at the core, $\tilde{c}_0(t)$, which appears in the definition (4.4). This is achieved by deriving a similar boundary value problem to the one satisfied by $u_i(r)$ (or, equivalently $u_{i,0}(r)$) given in Eqs. (3.7)–(3.13). Applying the linear operator $\mathcal{L}$ in Eq. (3.5) to Eq. (4.5) and utilising Eqs. (2.1)–(2.3) yields:

$$\frac{D_i}{r^2}\frac{\mathrm{d}}{\mathrm{d}r}\left(r^2\frac{\mathrm{d}u_{i,k}}{\mathrm{d}r}\right) = \frac{1}{C_0}\int_0^\infty t^k \frac{\partial c_i}{\partial t}\,\mathrm{d}t. \tag{4.10}$$

Integrating by parts and noting that $c_i(r, t) \to 0$ exponentially as $t \to \infty$ produces the following differential equation for $u_{i,k-1}(r)$:

$$\frac{D_i}{r^2}\frac{\mathrm{d}}{\mathrm{d}r}\left(r^2\frac{\mathrm{d}u_{i,k}}{\mathrm{d}r}\right) = -k u_{i,k-1}, \tag{4.11}$$

involving the $(k-1)$th moment at r, namely $u_{i,k-1}(r)$. Similar boundary and interlayer conditions to those in Eqs. (3.7)–(3.13) apply [14] giving the following boundary value problem for the kth moment:

$$\frac{D_0}{r^2}\frac{\mathrm{d}}{\mathrm{d}r}\left(r^2\frac{\mathrm{d}u_{0,k}}{\mathrm{d}r}\right) = -k u_{0,k-1}, \quad r \in (0, R_0), \tag{4.12}$$

$$\frac{D_i}{r^2}\frac{\mathrm{d}}{\mathrm{d}r}\left(r^2\frac{\mathrm{d}u_{i,k}}{\mathrm{d}r}\right) = -k u_{i,k-1}, \quad r \in (R_{i-1}, R_i), \quad i = 1, \ldots, n, \tag{4.13}$$

$$\frac{D_e}{r^2}\frac{\mathrm{d}}{\mathrm{d}r}\left(r^2\frac{\mathrm{d}u_{e,k}}{\mathrm{d}r}\right) = -k u_{e,k-1}, \quad r \in (R_n, R_\infty), \tag{4.14}$$

$$\frac{\mathrm{d}u_{0,k}}{\mathrm{d}r} = 0, \quad r = 0, \tag{4.15}$$

$$u_{i,k} = \sigma_i u_{i+1,k}, \quad D_i\frac{\mathrm{d}u_{i,k}}{\mathrm{d}r} = D_{i+1}\frac{\mathrm{d}u_{i+1,k}}{\mathrm{d}r}, \quad r = R_i, \quad i = 0, 1, \ldots, n-1, \tag{4.16}$$

$$D_n\frac{\mathrm{d}u_{n,k}}{\mathrm{d}r} = D_e\frac{\mathrm{d}u_{e,k}}{\mathrm{d}r}, \quad D_e\frac{\mathrm{d}u_{e,k}}{\mathrm{d}r} = P(\sigma_n u_{e,k} - u_{n,k}), \quad r = R_n, \tag{4.17}$$

$$u_{e,k} = 0, \quad r = R_\infty. \tag{4.18}$$

The release time is computed iteratively by solving the sequence of boundary value problems (4.12)–(4.18) for increasing values of k [18,20]. First, an initial estimate of t_r^* is calculated by setting $k = 1$ in Eq. (4.9), solving Eqs. (4.12)–(4.18) with $k = 1$ for $u_{0,1}(r)$ to give $\mathcal{M}_1 = u_{0,1}(0)$ and using the zeroth order moment computed previously (Section 3). Next, an improved estimate of t_r^* is computed by setting $k = 2$ in Eq. (4.9), solving Eqs. (4.12)–(4.18) with $k = 2$ for $u_{0,2}(r)$ to give $\mathcal{M}_2 = u_{0,2}(0)$ and using the previously computed first moment. The process repeats by increasing k until the value of t_r^* converges sufficiently to an accurate estimate of t_r as defined in Eq. (3.1). We remark that numerically solving the system (4.12)–(4.18) is computationally inexpensive, since the coefficient matrix that arises from spatial discretisation of the boundary value problem remains unchanged throughout the iterations and only needs to be factorized once, with only the right-hand side of Eqs. (4.12)–(4.14) changing with k.

5. Results and discussion

In this section, we apply the release time estimates of Sections 3 and 4 to several test cases. For all our numerical experiments we consider the drug diffusion model (2.1)–(2.10) with $n = 1$ (*core-shell model*) and the following base values for the geometrical and physical parameters [8,9,21]:

$$R_0 = 1.5{\cdot}10^{-3}\,\mathrm{m}, \quad R_1 = 1.7{\cdot}10^{-3}\,\mathrm{m}, \quad R_\infty = 30{\cdot}10^{-3}\,\mathrm{m}, \tag{5.1}$$

$$D_0 = 30{\cdot}10^{-11}\,\mathrm{m^2 s^{-1}}, \quad D_1 = 5{\cdot}10^{-11}\,\mathrm{m^2 s^{-1}}, \quad D_e = 30{\cdot}10^{-11}\,\mathrm{m^2 s^{-1}}, \tag{5.2}$$

$$\sigma_0 = \sigma_1 = 1, \quad P \to \infty. \tag{5.3}$$

Using this set of parameter values, we first investigate the convergence behaviour of the asymptotic estimate of the release time, t_r^* (4.9), for increasing values of k. In Table 1, we report the value of t_r^* and $\tilde{c}_0(t_r^*)$ for $k = 1, \ldots, 14$ and $\varepsilon = 10^{-4}, 10^{-5}, 10^{-6}$. These results show that t_r^* is converging to a highly accurate estimate of the release time, with $\lim_{k\to\infty}\tilde{c}_0(t_r^*)$ close to the prescribed value of ε (3.1) in all three cases. For the two smaller values of ε, $\lim_{k\to\infty}\tilde{c}_0(t_r^*)$ is closer to the specified value of ε because the one-term approximation (4.2) becomes more accurate for larger values of t. For this parameter set, the release time estimate converges to the second by $k = 12$ for all three values of ε.

We now investigate the sensitivity of t_r^* when varying the outer radius of the capsule, R_1, the mass transfer coefficient at the external coating, P, the diffusivity in the core, D_0, and the diffusivity in the hydrogel layer, D_1, about the base values Eqs. (5.1)–(5.3). Each of the parameters, R_1, P, D_0 and D_1, are varied one at a time holding the other three parameters fixed at the base values. We consider three values of R_1 between $1.52{\cdot}10^{-3}$ and $6{\cdot}10^{-3}$, P between $5{\cdot}10^{-8}$ and $5{\cdot}10^{-6}$, D_0 between $5{\cdot}10^{-11}$ and $5{\cdot}10^{-9}$ and D_1 between $5{\cdot}10^{-12}$ and $5{\cdot}10^{-10}$. In total, there are 12 test cases as labelled in Table 2 with the release time estimate t_r^* (4.9) calculated with $k = 15$ and $\varepsilon = 10^{-4}$ in all cases. In Fig. 3, for each test case, we plot the temporal profile of the dimensionless concentration at the centre of the capsule $\tilde{c}_0(t)$ to show the effect of varying R_1, P, D_0 and D_1. These results show that over the specified ranges of each parameter the time required for $\tilde{c}_0(t)$ to approach zero increases for increasing values of R_1 and decreasing values of P, D_0 and D_1 (Fig. 3). In Table 2, this translates to larger values of t_r^* for increasing values of R_1 and decreasing values of P, D_0 and D_1.

For each concentration curve in Fig. 3 we also indicate the result of applying the crude approximation of the release time $\hat{t}_r$ (3.27) using a vertical dash line. These results demonstrate that the crude approximation provides an accurate visual match with the time required to reach steady state. This is further confirmed in Table 2, which shows that for all 12 test cases $\tilde{c}_0(\hat{t}_r)$ is of the order 10^{-2}–10^{-3}. In this table, the zeroth and first moments, $\mathcal{M}_0$ and $\mathcal{M}_1$, are also given for each test case. Comparing cases 3 and 4 we see the importance of incorporating the first moment: both cases have a similar value for the zeroth moment, however, the heavy tail of case 3, evident in Fig. 3, leads to a significantly larger release time, which is appropriately captured by the significantly larger value for the first moment (see Table 2). In summary, although $\hat{t}_r$ is less precise than t_r^*, it is much easier to compute and can be useful to assess the release performance for different configurations.

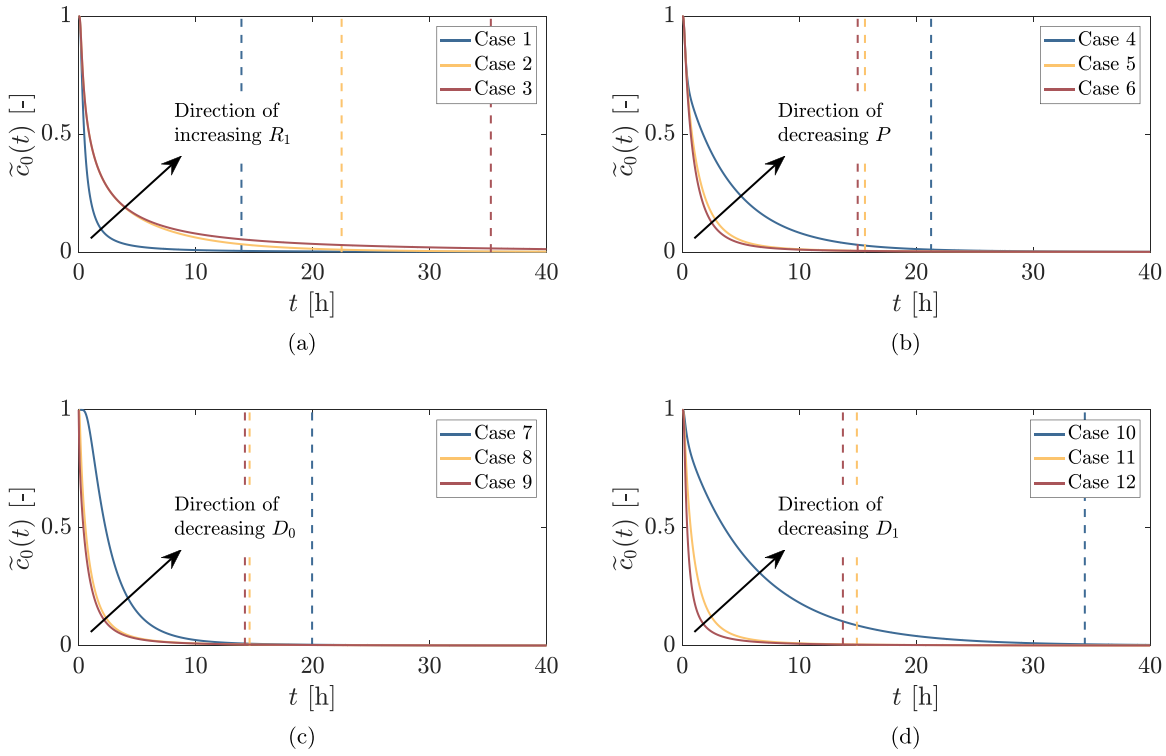

Fig. 3. Profiles of the dimensionless concentration at the centre of the capsule, $\tilde{c}_0(t)$, over time showing the effect of varying (a) the outer radius of the capsule (R_1); (b) the mass transfer coefficient at the external coating (P); (c) the diffusivity in the core (D_0); and (d) the diffusivity in the hydrogel layer (D_1). The vertical dash lines represent the corresponding crude approximation to the release time $\hat{t}_r$ (3.27). When varying a parameter all other variables are held fixed at the values given in Eqs. (5.1)–(5.3). All results are based on the drug diffusion model (2.1)–(2.10) with a single hydrogel layer ($n = 1$). The test cases match those reported in Table 2.

6. Conclusions

Polymer capsules, pellets, tablets, layer-by-layer vehicles and other micro-engineered drug releasing implants are attracting a great deal of attention for their potential use for therapeutic applications. The design of such novel drug delivery devices poses major challenges, such as the unknown significance of process parameters. Modelling and computational tools, however, can assist in designing drug delivery devices to enable control over the delivery rate and the time required to establish a steady-state flux. Moreover, the performance of a composite microcapsule can be sensibly enhanced if the release mechanism is understood and an appropriate mathematical model is used to characterize the releasing ability of the system. In this study, novel approaches to estimate the release time of diffusion problems from spherical multilayer capsules are presented under a limited number of physical assumptions. The method is based on the linearity of a pure diffusive system, that holds or dominates in most circumstances. No explicit solution of the diffusion problem is required; instead temporal moments of the drug concentration versus time curve at the centre of the capsule are used to derive analytical expressions that provide *a priori* quantitative indication of the drug release time. The proposed methodology, which accounts for the relevant geometrical and physical parameters, provides a simple tool to measure microcapsule dynamic performance.

Table 1
Convergence of the asymptotic estimate of the release time t_r^* (4.9) for increasing values of the index k applied to the drug diffusion model (2.1)–(2.10) with a single hydrogel layer ($n = 1$) and the physical parameters Eqs. (5.1)–(5.3). The value of t_r^* is calculated using three different choices for ε and is displayed in the format days:hours:minutes:seconds.

	$\varepsilon = 10^{-4}$		$\varepsilon = 10^{-5}$		$\varepsilon = 10^{-6}$	
k	t_r^*	$\tilde{c}_0(t_r^*)$	t_r^*	$\tilde{c}_0(t_r^*)$	t_r^*	$\tilde{c}_0(t_r^*)$
1	02:06:22:59	$7.2152 \cdot 10^{-4}$	02:22:53:05	$4.8197 \cdot 10^{-4}$	03:15:23:12	$3.5016 \cdot 10^{-4}$
2	07:23:03:31	$8.6792 \cdot 10^{-5}$	13:02:30:33	$2.0023 \cdot 10^{-5}$	18:05:57:35	$4.6400 \cdot 10^{-6}$
3	07:21:39:42	$8.8261 \cdot 10^{-5}$	15:11:32:11	$1.0190 \cdot 10^{-5}$	23:01:24:40	$1.1822 \cdot 10^{-6}$
4	07:14:19:34	$9.6411 \cdot 10^{-5}$	15:14:06:10	$9.8849 \cdot 10^{-6}$	23:13:52:46	$1.0199 \cdot 10^{-6}$
5	07:11:49:55	$9.9360 \cdot 10^{-5}$	15:13:37:58	$9.9401 \cdot 10^{-6}$	23:15:26:02	$1.0013 \cdot 10^{-6}$
6	07:11:02:47	$1.0031 \cdot 10^{-4}$	15:13:18:53	$9.9777 \cdot 10^{-6}$	23:15:34:58	$9.9953 \cdot 10^{-7}$
7	07:10:48:25	$1.0060 \cdot 10^{-4}$	15:13:11:17	$9.9926 \cdot 10^{-6}$	23:15:34:10	$9.9969 \cdot 10^{-7}$
8	07:10:44:09	$1.0069 \cdot 10^{-4}$	15:13:08:41	$9.9977 \cdot 10^{-6}$	23:15:33:14	$9.9988 \cdot 10^{-7}$
9	07:10:42:54	$1.0071 \cdot 10^{-4}$	15:13:07:52	$9.9994 \cdot 10^{-6}$	23:15:32:50	$9.9996 \cdot 10^{-7}$
10	07:10:42:33	$1.0072 \cdot 10^{-4}$	15:13:07:37	$9.9999 \cdot 10^{-6}$	23:15:32:41	$9.9999 \cdot 10^{-6}$
11	07:10:42:27	$1.0072 \cdot 10^{-4}$	15:13:07:32	$1.0000 \cdot 10^{-5}$	23:15:32:38	$1.0000 \cdot 10^{-6}$
12	07:10:42:25	$1.0072 \cdot 10^{-4}$	15:13:07:31	$1.0000 \cdot 10^{-5}$	23:15:32:37	$1.0000 \cdot 10^{-6}$
13	07:10:42:25	$1.0072 \cdot 10^{-4}$	15:13:07:31	$1.0000 \cdot 10^{-5}$	23:15:32:37	$1.0000 \cdot 10^{-6}$
14	07:10:42:25	$1.0072 \cdot 10^{-4}$	15:13:07:31	$1.0000 \cdot 10^{-5}$	23:15:32:37	$1.0000 \cdot 10^{-6}$

Table 2
Sensitivity of the asymptotic estimate of the release time, t_r^* with $\varepsilon = 10^{-4}$ and $k = 15$, and the crude approximation of the release time, $\hat{t}_r$, when varying the outer radius of the capsule (R_1); the mass transfer coefficient at the external coating (P); the diffusivity in the core (D_0); and the diffusivity in the hydrogel layer (D_1). When varying a parameter all other parameters are held fixed at the base values given in Eqs. (5.1)–(5.3). All results are based on the drug diffusion model (2.1)–(2.10) with a single hydrogel layer ($n = 1$). The test cases match those reported in Fig. 3.

Case	1	2	3	Case	4	5	6
R_1 [m]	$1.52 \cdot 10^{-3}$	$3.00 \cdot 10^{-3}$	$6.00 \cdot 10^{-3}$	P [m s^{-1}]	$5.00 \cdot 10^{-8}$	$5.00 \cdot 10^{-7}$	$5.00 \cdot 10^{-6}$
$\mathcal{M}_0$ [h]	1.05	2.74	3.61	$\mathcal{M}_0$ [h]	3.58	1.63	1.44
$\mathcal{M}_1$ [h^2]	18.39	43.30	111.17	$\mathcal{M}_1$ [h^2]	34.80	21.74	20.43
$\hat{t}_r$ [h]	13.92	22.48	35.24	$\hat{t}_r$ [h]	21.27	15.62	15.00
t_r^* [h]	177.80	188.55	237.58	t_r^* [h]	185.23	179.35	178.77
$\tilde{c}_0(\hat{t}_r)$ [-]	$5.38 \cdot 10^{-3}$	$1.06 \cdot 10^{-2}$	$1.59 \cdot 10^{-2}$	$\tilde{c}_0(\hat{t}_r)$ [-]	$1.09 \cdot 10^{-2}$	$5.50 \cdot 10^{-3}$	$5.43 \cdot 10^{-3}$
$\tilde{c}_0(t_r^*)$ [-]	$1.01 \cdot 10^{-4}$	$1.01 \cdot 10^{-4}$	$1.05 \cdot 10^{-4}$	$\tilde{c}_0(t_r^*)$ [-]	$1.01 \cdot 10^{-4}$	$1.01 \cdot 10^{-4}$	$1.01 \cdot 10^{-4}$
	(a) Varying R_1				(b) Varying P		

Case	7	8	9	Case	10	11	12
D_0 [m^2 s^{-1}]	$5.00 \cdot 10^{-11}$	$5.00 \cdot 10^{-10}$	$5.00 \cdot 10^{-9}$	D_1 [m^2 s^{-1}]	$5.00 \cdot 10^{-12}$	$5.00 \cdot 10^{-11}$	$5.00 \cdot 10^{-10}$
$\mathcal{M}_0$ [h]	3.15	1.28	1.09	$\mathcal{M}_0$ [h]	5.83	1.42	0.97
$\mathcal{M}_1$ [h^2]	31.39	19.76	19.14	$\mathcal{M}_1$ [h^2]	90.83	20.29	18.09
$\hat{t}_r$ [h]	19.96	14.61	14.22	$\hat{t}_r$ [h]	34.42	14.93	13.73
t_r^* [h]	181.17	178.51	178.25	t_r^* [h]	189.86	178.71	177.63
$\tilde{c}_0(\hat{t}_r)$ [-]	$4.47 \cdot 10^{-3}$	$5.47 \cdot 10^{-3}$	$5.54 \cdot 10^{-3}$	$\tilde{c}_0(\hat{t}_r)$ [-]	$6.49 \cdot 10^{-3}$	$5.42 \cdot 10^{-3}$	$5.38 \cdot 10^{-3}$
$\tilde{c}_0(t_r^*)$ [-]	$1.01 \cdot 10^{-4}$	$1.01 \cdot 10^{-4}$	$1.01 \cdot 10^{-4}$	$\tilde{c}_0(t_r^*)$ [-]	$1.01 \cdot 10^{-4}$	$1.01 \cdot 10^{-4}$	$1.01 \cdot 10^{-4}$
	(c) Varying D_0				(d) Varying D_1		

Declarations of interest

None.

Acknowledgments

G.P. acknowledges funding from the European Research Council under the European Unions Horizon 2020 Framework Programme (No.FP/2014-2020)/ERC Grant Agreement No. 739964 (COPMAT).

Supplementary material

Supplementary material associated with this article can be found, in the online version, at 10.1016/j.mbs.2019.108216.

References

[1] A. Larrañaga, M. Lomora, J.R. Sarasua, C.G. Palivan, A. Pandit, Polymer capsules as micro-/nanoreactors for therapeutic applications: current strategies to control membrane permeability, Prog. Mater. Sci. 90 (2017) 325–357.
[2] A.S. Timin, D.J. Gould, G.B. Sukhorukov, Multi-layer microcapsules: fresh insights and new applications, Exp. Op. Drug Deliv. 14 (5) (2017) 583–587.
[3] Y. Zhang, H.F. Chan, K.W. Leong, Advanced materials and processing for drug delivery: the past and the future, Adv. Drug Deliv. Rev. 65 (2013) 104–120.
[4] D. Lensen, K. van Breukelen, D.M. Vriezema, J.C. van Hest, Preparation of biodegradable liquid core PLLA microcapsules and hollow PLLA microcapsules using microfluidics, Macromol. Biosci. 10 (2010) 475–480.
[5] F. Cuomo, A. Ceglie, A. De Leonardis, F. Lopez, Polymer capsules for enzymatic catalysis in confined environments, Catalysts 9 (1) (2019), https://doi.org/10.3390/catal9010001.
[6] D.Y. Arifin, L.Y. Lee, C.H. Wang, Mathematical modeling and simulation of drug release from microspheres: implications to drug delivery systems, Adv. Drug Deliv. Rev. 58 (2006) 1274–1325.
[7] J.K. Tavares, A.A.U. de Souza, Modeling of the controlled release of betacarotene into anhydrous ethanol from microcapsules, OpenNano 1 (2016) 25–35.
[8] B. Kaoui, M. Lauricella, G. Pontrelli, Mechanistic modelling of drug release from multilayer capsules, Comput. Biol. Med. 93 (2018) 149–157.
[9] E.J. Carr, G. Pontrelli, Modelling mass diffusion for a multi-layer sphere immersed in a semi-infinite medium: application to drug delivery, Math. Biosci. 303 (2018) 1–9.
[10] R. Collins, The choice of an effective time constant for diffusive processes in finite systems, J. Phys. D 13 (1980) 1935–1947.
[11] L. Simon, Timely drug delivery from controlled-release devices: dynamic analysis and novel design concepts, Math. Biosci. 217 (2009) 151–158.
[12] G. Pontrelli, L. Simon, The choice of a performance indicator of release in transdermal drug delivery systems, in: P. Wriggers, T. Lenarz (Eds.), Biomedical Technology: Modeling, Experiments and Simulation, Springer International Publishing, 2018, pp. 49–64.
[13] K. Landman, M. McGuinness, Mean action time for diffusive processes, J. Appl. Math. Decis. Sci. 4 (2) (2000) 125–141.
[14] E.J. Carr, Characteristic timescales for diffusion processes through layers and across interfaces, Phys. Rev. E 97 (2018) 042115.
[15] M.J. Simpson, F. Jazaei, T.P. Clement, How long does it take for aquifer recharge or aquifer discharge processes to reach steady state? J. Hydrol. 501 (2013) 241–248.
[16] A. McNabb, G.C. Wake, Heat conduction and finite measures for transition times between steady states, IMA J. Appl. Math. 47 (2) (1991) 193–206.
[17] F. de Monte, J.V. Beck, D.E. Amos, Diffusion of thermal disturbances in two-dimensional cartesian transient heat conduction, Int. J. Heat Mass Transf. 51 (2008) 5931–5941.
[18] E.J. Carr, Calculating how long it takes for a diffusion process to effectively reach steady state without computing the transient solution, Phys. Rev. E 96 (2017) 012116.
[19] L. Simon, J. Ospina, On the effusion time of drugs from the open pore of a spherical vesicle, Physica A 451 (2016) 366–372.
[20] E.J. Carr, M.J. Simpson, Accurate and efficient calculation of response times for groundwater flow, J. Hydrol. 558 (2018) 470–481.
[21] S. Henning, D. Edelhoff, B. Ernst, S. Leick, H. Rehage, D. Suter, Characterizing permeability and stability of microcapsules for controlled drug delivery by dynamic NMR microscopy, J. Magn. Reson. 221 (2012) 11–18.
[22] J. Crank, The Mathematics of Diffusion, Oxford Univ. Press, 1975.
[23] G. Pontrelli, F. de Monte, A multi-layer porous wall model for coronary drug-eluting stents, Int. J. Heat Mass Transf. 53 (2010) 3629–3637.
[24] F. Pukelsheim, The three sigma rule, Am. Stat. 48 (2) (1994) 88–91.